

Study of stacking interactions between two neutral tetrathiafulvalene molecules in Cambridge Structural Database crystal structures and by quantum chemical calculations

Ivana S. Antonijević,^a Dušan P. Malenov,^{b,c} Michael B. Hall^d and Snežana D. Zarić^{b,c,*}

Received 8 August 2018

Accepted 2 November 2018

Edited by A. Nangia, CSIR–National Chemical Laboratory, India

Keywords: tetrathiafulvalene; stacking; Cambridge Structural Database; interaction energies; CCSD(T)/CBS.

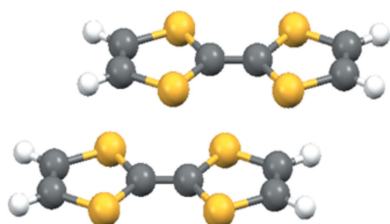
Supporting information: this article has supporting information at journals.iucr.org/b

^aInstitute of Chemistry, Technology and Metallurgy, University of Belgrade, Njegoševa 12, Belgrade, 11000, Serbia, ^bFaculty of Chemistry, University of Belgrade, Studentski trg 12-16, Belgrade, 11000, Serbia, ^cDepartment of Chemistry, Texas A&M University at Qatar, PO Box 23874, Doha, Qatar, and ^dDepartment of Chemistry, Texas A&M University, College Station, Texas 77843-3255, USA. *Correspondence e-mail: szaric@chem.bg.ac.rs

Tetrathiafulvalene (TTF) and its derivatives are very well known as electron donors with widespread use in the field of organic conductors and superconductors. Stacking interactions between two neutral TTF fragments were studied by analysing data from Cambridge Structural Database crystal structures and by quantum chemical calculations. Analysis of the contacts found in crystal structures shows high occurrence of parallel displaced orientations of TTF molecules. In the majority of the contacts, two TTF molecules are displaced along their longer C_2 axis. The most frequent geometry has the strongest TTF–TTF stacking interaction, with CCSD(T)/CBS energy of -9.96 kcal mol⁻¹. All the other frequent geometries in crystal structures are similar to geometries of the minima on the calculated potential energy surface.

1. Introduction

Tetrathiafulvalene (TTF) is an organosulfur compound of great importance for the development of ‘organic metals’, non-metallic materials that can be used as organic conductors and superconductors because of their high electrical conductivity (Martín, 2013). Since discovering the first organic conductors, TTFCl (Wudl *et al.*, 1972) and the first charge-transfer (CT) complex TTF–TCNQ (TCNQ = tetracyanoquinodimethane) (Ferraris *et al.*, 1973), TTF has been among the most studied heterocyclic systems (Yamada & Sugimoto, 2004; Bendikov *et al.*, 2004). TTF and its derivatives have been extensively studied as building blocks for charge-transfer salts, but also as constructors of supramolecular structures including different materials with electrical, magnetic and optical properties, especially molecular machines (Martín, 2013; Bendikov *et al.*, 2004; Frère & Skabara, 2005; Otsubo & Takimiya, 2004; Bryce, 2000; Segura & Martín, 2001; Nielsen *et al.*, 2000; Ziganshina *et al.*, 2004; Canevet *et al.*, 2009; Brunetti *et al.*, 2012; Jiang *et al.*, 2014). Moreover, TTF can be used to functionalize graphene (Kaminska *et al.*, 2012; Varghese *et al.*, 2009), which might be very important in the research on amyloid-based neurodegenerative diseases. It has been shown that graphene–amyloid stacks can be more stable than amyloid–amyloid stacks (Božinovski *et al.*, 2018), which are essential for the molecular recognition and self-assembly processes that lead to amyloid formation (Gazit, 2002; Bemporad *et al.*, 2006; Ninković *et al.*, 2017).



Parallel packing is very common in crystal structures containing a TTF unit. In the solid state, TTF and its derivatives tend to form highly ordered structures through π - π and S \cdots S interactions (Rovira & Novoa, 1999). Formation of π - π stacking, S \cdots S and C—H \cdots S interactions enable charge transfer in organic transistors containing a TTF constituent (Jiang *et al.*, 2014). A combined statistical and *ab initio* study has shown that attractive S \cdots S interactions between TTF fragments contribute to stabilizing the crystal structure (Rovira & Novoa, 1999). This is in agreement with our results on S \cdots S interactions between cysteine fragments, which suggest that the most dominant geometries in crystal structures are those with parallel orientation (Antonijević *et al.*, 2016). Calculated CCSD(T)/CBS interaction energies show that the most stable geometry with parallel S \cdots S interaction has an interaction energy of $-1.80 \text{ kcal mol}^{-1}$ ($1 \text{ kcal mol}^{-1} = 4.184 \text{ kJ mol}^{-1}$) (Antonijević *et al.*, 2016).

Until now, stacking interactions between two TTF cation radicals have been theoretically and experimentally studied (Wang *et al.*, 2009, 2011; Fumanal *et al.*, 2013; Garcia-Yoldi *et al.*, 2009; Rosokha & Kochi, 2007; Capdevila-Cortada *et al.*, 2014). Two TTF $^{\bullet+}$ cation radicals can interact to form an intermolecular covalent bonding interaction. In dimers consisting of two TTF cation radicals multicenter bonding was observed in the solid state as well as in solution. Theoretical studies show that a dimer is stabilized with electrostatic \cdots cation/anion interactions from the surroundings which are further supported by a dispersion component (Garcia-Yoldi *et al.*, 2009).

Stacking interactions are typical for aromatic molecules and they have been extensively investigated (Salonen *et al.*, 2011; Lee *et al.*, 2007; Ninković *et al.*, 2011; Sinnokrot *et al.*, 2002; Raju *et al.*, 2011). The most stable stacking interaction for a benzene dimer is a parallel displaced geometry at an offset (horizontal displacement) r , of 1.51 \AA , with an interaction energy of $-2.73 \text{ kcal mol}^{-1}$ (Lee *et al.*, 2007). Our previous work showed that stacking interactions between aromatic molecules can be substantial at unusually large offset values (Ninković *et al.*, 2011). At the 4.5 \AA offset, the benzene-benzene stacking interaction energy is $-2.01 \text{ kcal mol}^{-1}$ and these interactions are highly dominant in crystal structures (Ninković *et al.*, 2011). In addition, the work in our group showed substantial stacking interactions of non-aromatic moieties, such as chelate rings (Malenov & Zarić, 2018; Malenov *et al.*, 2017), cyclohexane (Ninković *et al.*, 2016) and hydrogen-bridged rings (Blagojević *et al.*, 2017; Blagojević & Zarić, 2015). Stacking interactions of all these moieties are comparable in energy with stacking interactions of aromatic molecules and some of them are significantly stronger. Stacking arrangements of entire blocks of non-aromatic molecules (Mora *et al.*, 2017) and even non-cyclic molecules (Czech *et al.*, 2017) can also be found in crystal structures.

There are studies showing that geometries of stacking interactions between TTF fragments influence the conductivity properties of TTF-based materials (Kobayashi *et al.*, 1983; Coronado & Day, 2004). However, it is interesting to see if energies of stacking interactions of non-aromatic TTF rings

are comparable with those of aromatic rings. Therefore, we present our detailed study of stacking interactions between two neutral TTF fragments, including geometries in the crystal structures from Cambridge Structural Database and quantum chemical calculations on stacking interaction energies. Quantum chemical calculations were performed using several methods, ω B97xD density functional (Chai & Head-Gordon, 2008), B2PLYP-D3BJ (Grimme *et al.*, 2010, 2011; Goerigk & Grimme, 2011) density functional SAPT (Jeziorski *et al.*, 1994) energy decomposition analysis and the very accurate CCSD(T) method (Raghavachari *et al.*, 1989) at the complete basis set as the gold standard of quantum chemistry (Sinnokrot *et al.*, 2002). To the best of our knowledge, this is the first study describing the preferred geometries and interaction energies between two neutral stacked TTF fragments.

2. Methodology

2.1. CSD search

The search of Cambridge Structural Database (CSD; Version 5.39, November 2017) (Allen, 2002; Groom *et al.*, 2016) was performed using the program *ConQuest* (Version 1.20; Bruno *et al.*, 2002) to extract all structures containing stacking contacts between two TTF fragments and satisfying selected geometrical criteria. The geometrical parameters used to search CSD and to characterize the TTF-TTF interactions are displayed in Fig. 1. The CSD search considered all the contacts between two neutral molecules containing TTF fragments, with the angle between their mean planes (P and P') smaller than 10° , and distance d between the centroids of their exocyclic double bonds shorter than 10.0 \AA . The contact was considered a TTF-TTF stacking interaction if at least one distance between centers of two five-membered rings (d_1) was

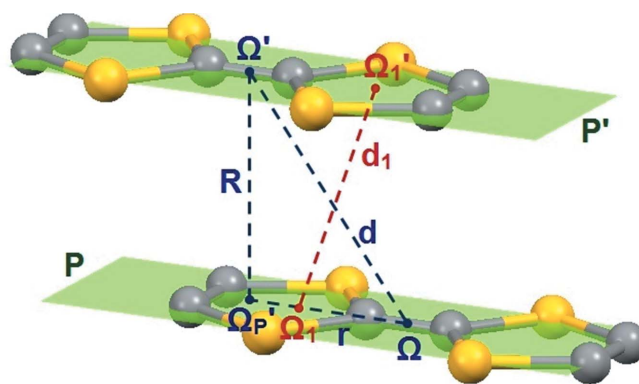


Figure 1
Geometrical parameters used to describe stacking interactions between two TTF fragments: P and P' are the average planes of interacting fragments; d is the distance between the centers of two C=C double bonds (Ω and Ω'), while d_1 is the shortest distance between the centroids of two interacting five-membered rings (Ω_1 and Ω_1'). Normal distance R is the distance between centroid Ω' and its projection $\Omega_{p'}$ onto the P plane. Horizontal displacement r is the distance between the centroid Ω and the projection $\Omega_{p'}$. The torsion angle defining the orientation of TTF fragments is defined by centroids: Ω_1 - Ω - Ω' - Ω_1' .

shorter than 5.0 Å and the normal distance R between mean planes of the fragments was shorter than 4.0 Å.

2.2. Quantum chemical calculations

All calculations were performed using the *Gaussian09* (Frisch *et al.*, 2013) program package. Unsubstituted TTF was used as the model molecule for calculating TTF stacking interaction energies. The geometry of the TTF monomer was optimized using the ω B97xD density functional (Chai & Head-Gordon, 2008) and the def2-TZVP basis set (Weigend & Ahlrichs, 2005), and confirmed as a true minimum by performing the calculations of vibrational frequencies.

For several stacking geometries CCSD(T) interaction energies at the complete basis set (CBS) (Sinnokrot & Sherrill, 2004) were calculated by applying the extrapolation scheme proposed by Mackie & DiLabio (2011) (see supporting information). Due to high computational demands of CCSD(T)/CBS, potential energy surfaces for TTF–TTF stacking were calculated using the less demanding B2PLYP-D3BJ/6-311++G** level (Grimme *et al.*, 2010, 2011; Goerigk & Grimme, 2011; Krishnan *et al.*, 1980; Clark *et al.*, 1983), which is in good agreement with CCSD(T)/CBS (supporting information). The energies of minima on potential energy curves were calculated with CCSD(T)/CBS level.

Energy decomposition analysis of interaction energy minima was performed with the SAPT 2+3 method (Hohenstein & Sherrill, 2010) using def2-TZVP basis set (Weigend & Ahlrichs, 2005) in the *Psi4* (Parrish *et al.*, 2017) program package. This method calculates the overall interaction energy as a sum of electrostatic, dispersion, exchange and induction energies. Electrostatic potential of the tetrathiafulvalene molecule was mapped from its B2PLYP-D3BJ/6-311++G**

wavefunction on the 0.001 a.u. density surface (Bader *et al.*, 1987), using the *Wave Function Analysis–Surface Analysis Suite* (WFA-SAS) (Bulat *et al.*, 2010) program.

3. Results and discussion

3.1. Analysis of the data from crystal structures

Crystal structures from the CSD were studied by analyzing different geometrical parameters to determine geometrical characteristics of interactions between two unsubstituted TTF molecules. We searched Cambridge Structural Database (CSD) using the criteria described in §2.1. The CSD search derived 1279 stacking contacts between TTF molecules.

The mutual orientation of two TTF molecules is defined by the torsion angle (Fig. 1). The distribution of torsion angle values (Fig. S1) shows that the majority of contacts have a tendency towards the values of this angle in the range from 0° to 10° and from 170° to 180°. Due to symmetry of the TTF unit, these angles are equivalent, and indicate that longer C_2 axes of interacting fragments are parallel. These torsion angle values are present in 1212 interactions, which is 94.8% of all stacking interactions. The distribution of normal distance (R , Fig. 1) shows that most contacts have values of normal distance in the range from 3.5 to 3.6 Å (Fig. S2).

The density map of mutual orientations between TTF fragments with respect to offset r (Fig. 1) and its horizontal and vertical component (r_x , r_y , Fig. 2) has four highly populated areas with centers at points (0.00, 1.50), (0.00, 4.50), (1.75, 0.00) and (1.75, 3.50) (Fig. 2). Examples of crystal structures for each area are given in Fig. 3. By far the most frequent geometry is the type 1, the geometries of type 2 and type 4 have similar occurrences, while the geometry of type 3 is the least frequent of all four types (Fig. 2).

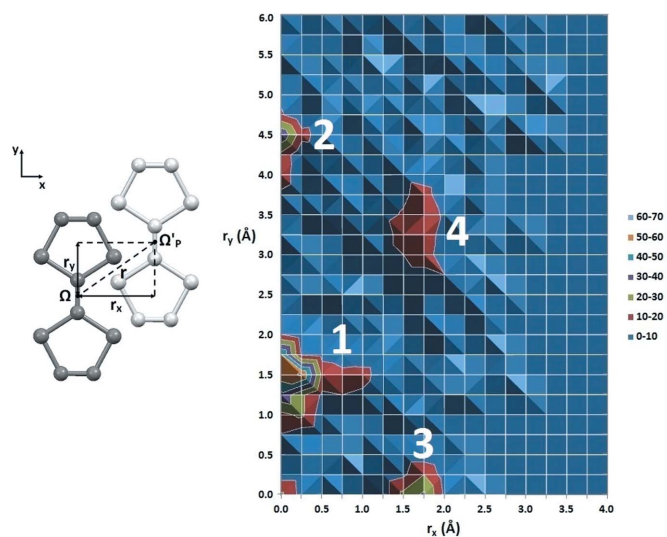


Figure 2

Density map with mutual orientations of stacked TTF fragments; the origin of the plot is the center of the C=C double bond of one molecule, while the map shows the position of the projection of the center of the C=C bond of the other molecule on the plane of the first one. The mutual orientation of two TTF fragments is defined by the horizontal (r_x) and vertical (r_y) component of the offset.

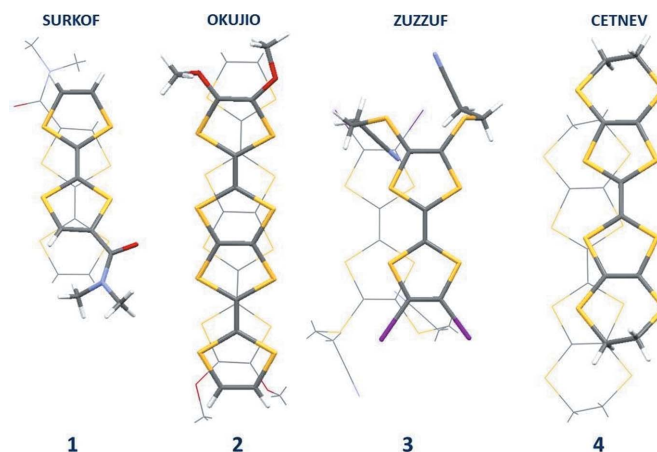


Figure 3

The most frequent stacking geometries between TTF fragments in the CSD. The CSD refcodes are given above each geometry (SURKOF: Batsanov *et al.*, 1995; OKUJIO: Ito *et al.*, 2011; ZUZZUF: Lieffrig *et al.*, 2014; CETNEV: Gomez-Garcia *et al.*, 2006). The numbers below the geometries indicate their positions on the density map in Fig. 2.

Table 1

Geometrical parameters and CCSD(T)/CBS and SAPT 2+3/def2-TZVP interaction energies of the most stable geometries (Fig. 5) for TTF–TTF stacking.

SAPT energies are decomposed into electrostatic (ES), exchange (EX), induction (IND) and dispersion (DISP) energies. All energies are given in kcal mol⁻¹.

Geometry	r_x (Å)	r_y (Å)	R (Å)	ΔE		ES	EX	IND	DISP	DISP + EX†
				CCSD(T) CBS	SAPT 2+3 def2-TZVP					
₂ Ymin	0.0	1.8	3.5	-9.96	-10.13	-7.25	18.70	-1.98	-19.60	-0.90
₁ Ymin	0.0	5.3	3.4	-6.74	-6.67	-5.83	11.10	-1.32	-10.62	0.48
₂ Xmin	1.7	0.0	3.5	-8.66	-8.74	-6.73	17.86	-1.69	-18.17	-0.31
₁ Xmin	1.3	4.1	3.5	-6.88	-6.74	-5.01	10.85	-1.16	-11.42	-0.57

† The sum of dispersion and exchange is known as ‘net dispersion’ (Hohenstein & Sherrill, 2009; Sherrill, 2013).

3.2. Interaction energies

Potential energy surfaces were calculated using model systems of two neutral TTF molecules (Fig. 4). For calculations, one TTF molecule was fixed, while the position of the other molecule is systematically changed by increasing the

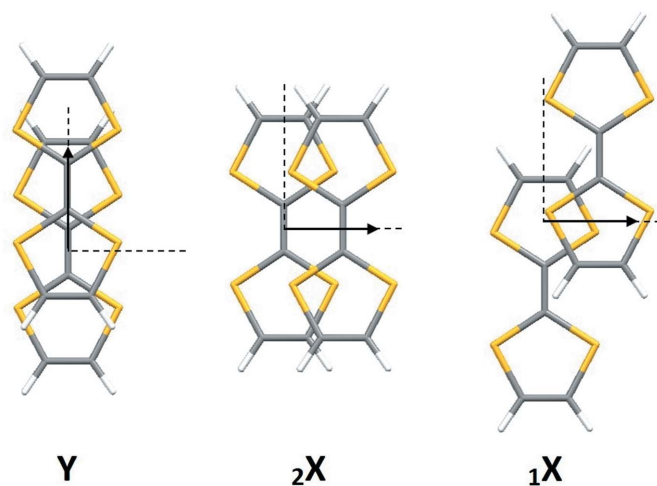


Figure 4
Model systems used for the calculations of TTF–TTF stacking interaction energies. In model system Y, the molecules are displaced along the long C_2 axes. In model systems ₂X and ₁X, the molecules are displaced along the short C_2 axes. The presented geometries have the offset values of 1.5 Å.

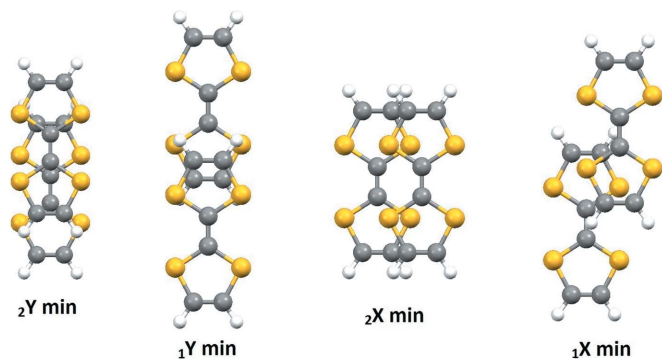


Figure 5
Geometries for minima found on interaction energy curves of TTF stacking for model systems Y, ₂X and ₁X, calculated at B2PLYP-D3BJ/6-311++G** level.

value of offset r . In two model systems (Y and ₂X, Fig. 4), the starting geometry was the one in which the TTF molecules are entirely overlapped. In the third model system (₁X), the starting geometry was the one in which only one ring of each TTF was involved in the overlapping (Fig. 4).

The strongest TTF–TTF stacking was calculated for the model system Y at $r = 1.8$ Å (geometry ₂Ymin, Fig. 5), with the CCSD(T)/CBS interaction energy of -9.96 kcal mol⁻¹ (Table 1). The Y curve has another minimum, at $r = 5.3$ Å (geometry ₁Ymin, Fig. 5), with the CCSD(T)/CBS interaction energy of -6.74 kcal mol⁻¹ (Table 1).

On the potential energy curve for model system ₂X only one minimum was obtained, at $r = 1.7$ Å (geometry ₂Xmin, Fig. 5). The CCSD(T)/CBS energy of this minimum is -8.66 kcal mol⁻¹ (Table 1). The potential energy curve for model system ₁X also reveals one minimum, at $r = 1.3$ Å (geometry ₁Xmin, Fig. 5). This minimum has the CCSD(T)/CBS interaction energy of -6.88 kcal mol⁻¹ (Table 1).

Data about stacking of TTF molecules indicate, as one can anticipate, that stacking is stronger if larger areas of molecules are involved in the stacking (Table 1, Fig. 5). Stacking interaction between two TTF molecules (-9.96 kcal mol⁻¹) is stronger than the stacking of two naphthalene molecules (-6.23 kcal mol⁻¹) (Rubeš *et al.*, 2008); naphthalene being an aromatic molecule of similar size to TTF.

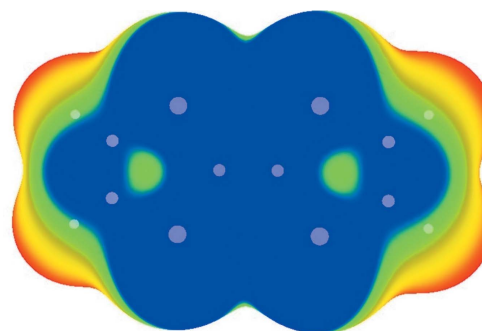


Figure 6
Computed B2PLYP-D3BJ/6-311++G** electrostatic potentials on the 0.001 a.u. surface of tetrathiafulvalene. Color ranges, in kcal mol⁻¹, are red, greater than 15.75; yellow, from 0.00 to 15.75; green, from 0.00 to -4.33 ; blue, more negative than -4.33 . The gray dots represent the atoms of TTF.

3.3. Energy decomposition analysis

The energy decomposition analysis for TTF–TTF stacking was performed with SAPT 2+3 method with def2-TZVP basis set because this level of theory is in good agreement with the CCSD(T)/CBS method (Table 1). SAPT analysis revealed that the most stable minima (${}_2\text{Ymin}$ and ${}_2\text{Xmin}$) are particularly stabilized by strong dispersion forces (Table 1), as large molecular areas overlap in these geometries. Dispersion is the strongest in ${}_2\text{Ymin}$, $-19.60 \text{ kcal mol}^{-1}$, while it is $-18.17 \text{ kcal mol}^{-1}$ in ${}_2\text{Xmin}$ (Table 1). Even though the dispersion is largely canceled by the repulsive exchange term in both minima, it is more preserved for ${}_2\text{Ymin}$ (see ‘net dispersion’ values in Table 1).

It can be noted that the electrostatic attraction is also the strongest in ${}_2\text{Ymin}$, because this geometry has reduced electrostatic repulsion between very negative electrostatic potentials above the sulfur atoms, which partially overlap with positive potentials at the edges of hydrogen atoms (Figs. 5 and 6). In the ${}_2\text{Xmin}$ geometry electrostatic attraction is significant, although somewhat smaller than in ${}_2\text{Ymin}$, because of less overlap of positive and negative potentials (Figs. 5 and 6).

For the less stable stacking minima, ${}_1\text{Ymin}$ and ${}_1\text{Xmin}$, both dispersion and electrostatic terms are less attractive than for ${}_2\text{Ymin}$ and ${}_2\text{Xmin}$ (Table 1). Dispersion interactions are less attractive, as smaller molecular areas overlap (Fig. 5). Dispersion terms are canceled by exchange terms as well, particularly for ${}_1\text{Ymin}$, which does not have favorable net dispersion (Table 1). However, this minimum has more favorable electrostatic interactions than ${}_1\text{Xmin}$ (Table 1) owing to more overlap of positive hydrogen edges with negative sulfur potentials (Figs. 5 and 6).

3.4. Comparing the geometries in the CSD and interaction energies

Data from both the crystal structures (Fig. 3) and the potential energy curves (Fig. 7) showed that TTF molecules form the strongest stacking interactions in parallel displaced geometries, which is typical for aromatic rings (Lee *et al.*, 2007;

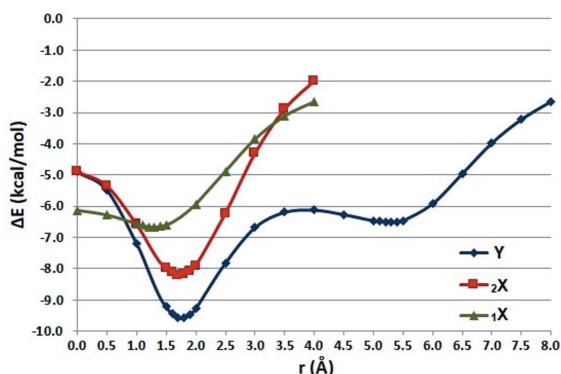


Figure 7

Potential energy curves for TTF–TTF stacking for model systems Y, ${}_2\text{X}$ and ${}_1\text{X}$ (Fig. 4) calculated at B2PLYP-D3BJ/6-311++G** level. The curves were obtained by changing the normal distances (R) for a series of offsets (r) and present the energies of the strongest interaction for each offset.

Ninković *et al.*, 2011), most of the chelate rings (Malenov & Zarić, 2018; Malenov *et al.*, 2017) and also hydrogen-bridged rings (Blagojević *et al.*, 2017; Blagojević & Zarić, 2015). The results of quantum chemical calculations are in very good agreement with the data found in the CSD crystal structures, which is well illustrated by similarities of the crystal structures in Fig. 3 and calculated minima on potential surface in Fig. 5.

The calculations were performed with non-substituted TTF molecules, while in crystal structures TTF molecules have substituents or they are fused with other rings. The most frequent TTF–TTF stacking geometries found in the CSD (type 1, Fig. 3), in which both rings of each TTF fragment participate in stacking, are very similar to the geometry with the strongest interaction (structure ${}_2\text{Ymin}$, Fig. 5). Another type of frequent TTF–TTF stacking geometry in the CSD, which is labeled as type 3 (Fig. 3), is very similar to another minimum at the potential energy surface (${}_2\text{Xmin}$, Fig. 5), with a somewhat weaker interaction energy of $-8.66 \text{ kcal mol}^{-1}$ (Table 1).

The other two frequent geometries in the CSD crystal structures (types 2 and 4, Fig. 3) are also similar to the minima found on potential energy curves (${}_1\text{Y}$ and ${}_1\text{X}$, Fig. 5). However, the offsets of crystal structure geometries are somewhat different from those from the potential curve minima, and we were able to determine why by the visual analysis of crystal structures.

The type 2 geometry of TTF–TTF stacking is typical for fused TTF fragments, and it appears alongside the type 1 geometry [structure OKUJIO (Ito *et al.*, 2011), Fig. 3]. Type 2 is therefore somewhat altered from the corresponding minimum (${}_1\text{Ymin}$) so that the geometry with the strongest interaction (type 1) can be formed. Moreover, the energy loss due to this alteration is very small, as the curve around this minimum is relatively flat (Fig. 7). Overall, this combined type 1 and type 2 stacking of fused fragments is very strong, and type 2 geometry is then more prevalent in crystal structures than type 3 (Fig. 2).

Type 4 geometry is typical for TTF fragments whose rings are fused with sulfur-containing six-membered rings [structure CETNEV (Gomez-Garcia *et al.*, 2006), Fig. 3]. In these structures, there are also two additional stacking interactions of TTF rings with fused six-membered rings (Fig. 3), which significantly contribute to stabilization of the overall stacks. In order for this additional stacking to form, type 4 is somewhat altered from the corresponding minimum ${}_1\text{Xmin}$. However, the energy loss due to this alteration is also very small, as the curve around this minimum is relatively flat (Fig. 7). The type 4 stacking is then altogether very strong and it occurs in the crystal structures more often than the stacking of type 3 (Fig. 2).

4. Conclusion

In this paper, stacking interactions between neutral TTF fragments have been systematically investigated by analyzing data from crystal structures archived in Cambridge Structural Database and by calculating their interaction energies with

quantum chemical methods. Results of the CSD search showed a great tendency towards parallel displaced stacking, which is the typical geometry of stacking interactions. The quantum chemical calculations determined that all the minima on the potential energy surface correspond to parallel displaced geometries. The most frequent TTF–TTF stacking geometry in crystal structures is the one with the strongest calculated interaction energy. The CCSD(T)/CBS energy of this interaction is $-9.96 \text{ kcal mol}^{-1}$, which is significantly stronger than the stacking between two naphthalene molecules ($-6.23 \text{ kcal mol}^{-1}$). The other frequent geometries in CSD crystal structures are identical or very similar to geometries at minima on the potential energy surface. The small difference of most frequent geometries in crystal structures and the calculated geometries of minima on the potential energy surface are a consequence of the difference in the non-substituted TTF model system used for calculations and real molecules in crystal structures. The TTF–TTF stacking interactions are highly dominated by dispersion forces, with electrostatic interactions also being prominent. Our findings on TTF–TTF stacking interactions could be of great importance in a variety of molecular systems containing the TTF unit.

Acknowledgements

The HPC resources and services used in this work were partially provided by the IT Research Computing group in Texas A&M University at Qatar. We thank Dr Horst Borrmann from the Max-Planck Institute for Chemical Physics of Solids in Dresden, Germany, for his support. ISA would like to thank DAAD for scholarship and financial support.

Funding information

The following funding is acknowledged: Serbian Ministry of Education, Science and Technological Development (grant No. 172065 to Snežana D. Zarić); Qatar National Research Fund (a member of the Qatar Foundation) (grant No. NPRP8-425-1-087 to Michael B. Hall); Qatar Foundation for Education, Science and Community Development (<http://www.qf.org.qa>) for IT research computing.

References

Allen, F. H. (2002). *Acta Cryst.* **B58**, 380–388.
 Antonijević, I. S., Janjić, G. V., Milčić, M. K. & Zarić, S. D. (2016). *Cryst. Growth Des.* **16**, 632–639.
 Bader, R. F. W., Carroll, M. T., Cheeseman, J. R. & Chang, C. (1987). *J. Am. Chem. Soc.* **109**, 7968–7979.
 Batsanov, A. S., Bryce, M. R., Heaton, J. N., Moore, A. J., Skabara, P. J., Howard, J. A. K., Orti, E., Viruela, P. M. & Viruela, R. (1995). *J. Mater. Chem.* **5**, 1689–1696.
 Bemporad, F., Taddei, N., Stefani, M. & Chiti, F. (2006). *Protein Sci.* **15**, 862–870.
 Bendikov, M., Wudl, F. & Perepichka, D. F. (2004). *Chem. Rev.* **104**, 4891–4946.
 Blagojević, J. P., Veljković, D. Ž. & Zarić, S. D. (2017). *CrystEngComm*, **19**, 40–46.
 Blagojević, J. P. & Zarić, S. D. (2015). *Chem. Commun.* **51**, 12989–12991.

Božinovski, D. M., Petrović, P. V., Belić, M. R. & Zarić, S. D. (2018). *ChemPhysChem*, **19**, 1226–1233.
 Brunetti, F. G., López, J. L., Atienza, C. & Martín, N. (2012). *J. Mater. Chem.* **22**, 4188–4205.
 Bruno, I. J., Cole, J. C., Edgington, P. R., Kessler, M., Macrae, C. F., McCabe, P., Pearson, J. & Taylor, R. (2002). *Acta Cryst.* **B58**, 389–397.
 Bryce, M. R. (2000). *J. Mater. Chem.* **10**, 589–598.
 Bulat, F. A., Toro-Labbé, A., Brinck, T., Murray, J. S. & Politzer, P. (2010). *J. Mol. Model.* **16**, 1679–1691.
 Canevet, D., Sallé, M., Zhang, G., Zhang, D. & Zhu, D. (2009). *Chem. Commun.* **45**, 2245–2269.
 Capdevila-Cortada, M., Miller, J. S. & Novoa, J. J. (2014). *Chem. Eur. J.* **20**, 7784–7795.
 Chai, J. D. & Head-Gordon, M. (2008). *Phys. Chem. Chem. Phys.* **10**, 6615–6620.
 Clark, T., Chandrasekhar, J., Spitznagel, G. W. & Schleyer, P. V. R. (1983). *J. Comput. Chem.* **4**, 294–301.
 Coronado, E. & Day, P. (2004). *Chem. Rev.* **104**, 5419–5448.
 Czech, C., Glinemann, J., Johansson, K. E., Bolte, M. & Schmidt, M. U. (2017). *Acta Cryst.* **B73**, 1075–1084.
 Ferraris, J., Cowan, D. O., Walatka, V. V. & Perlstein, J. H. (1973). *J. Am. Chem. Soc.* **95**, 948–949.
 Frère, P. & Skabara, P. (2005). *Chem. Soc. Rev.* **34**, 69–98.
 Frisch, M. J., Trucks, G. W., Schlegel, H. B., Scuseria, G. E., Robb, M. A., Cheeseman, J. R., Scalmani, G., Barone, V., Mennucci, B., Petersson, G. A., Nakatsuji, H., Caricato, M., Li, X., Hratchian, H. P., Izmaylov, A. F., Bloino, J., Zheng, G., Sonnenberg, J. L., Hada, M., Ehara, M., Toyota, K., Fukuda, R., Hasegawa, J., Ishida, M., Nakajima, T., Honda, Y., Kitao, O., Nakai, H., Vreven, T., Montgomery, J. A. Jr, Peralta, J. E., Ogliaro, F., Bearpark, M., Heyd, J. J., Brothers, E., Kudin, K. N., Staroverov, V. N., Kobayashi, R., Normand, J., Raghavachari, K., Rendell, Burant, A. J. C., Iyengar, S. S., Tomasi, J., Cossi, M., Rega, N., Millam, J. M., Klene, M., Knox, J. E., Cross, J. B., Bakken, V., Adamo, C., Jaramillo, J., Gomperts, R., Stratmann, R. E., Yazyev, O., Austin, A. J., Cammi, R., Pomelli, C., Ochterski, J. W., Martin, R. L., Morokuma, K., Zakrzewski, V. G., Voth, G. A., Salvador, P., Dannenberg, J. J., Dapprich, S., Daniels, A. D., Farkas, Ö., Foresman, J. B., Ortiz, J. V., Cioslowski, J. & Fox, D. J. (2013). *Gaussian09*, revision D.01, Gaussian, Inc., Wallingford, CT, USA.
 Fumanal, M., Capdevila-Cortada, M., Miller, J. S. & Novoa, J. J. (2013). *J. Am. Chem. Soc.* **135**, 13814–13826.
 Garcia-Yoldi, I., Miller, J. S. & Novoa, J. J. (2009). *J. Phys. Chem. A*, **113**, 484–492.
 Gazit, E. (2002). *FASEB J.* **16**, 77–83.
 Goerigk, L. & Grimme, S. (2011). *J. Chem. Theory Comput.* **7**, 291–309.
 Gomez-Garcia, C. J., Coronado, E., Curreli, S., Gimenez-Saiz, C., Deplano, P., Mercuri, M. L., Pilia, L., Serpe, A., Faulmann, C. & Canadell, E. (2006). *Chem. Commun.* **47**, 4931–4933.
 Grimme, S., Antony, J., Ehrlich, S. & Krieg, H. (2010). *J. Chem. Phys.* **132**, 154104.
 Grimme, S., Ehrlich, S. & Goerigk, L. (2011). *J. Comput. Chem.* **32**, 1456–1465.
 Groom, C. R., Bruno, I. J., Lightfoot, M. P. & Ward, S. C. (2016). *Acta Cryst.* **B72**, 171–179.
 Hohenstein, E. G. & Sherrill, C. D. (2009). *J. Phys. Chem. A*, **113**, 878–886.
 Hohenstein, E. G. & Sherrill, C. D. (2010). *J. Chem. Phys.* **133**, 014101.
 Ito, T., Nakamura, K., Shirahata, T., Kawamoto, T., Mori, T. & Misaki, Y. (2011). *Chem. Lett.* **40**, 81–83.
 Jeziorski, B., Moszynski, R. & Szalewicz, K. (1994). *Chem. Rev.* **94**, 1887–1930.
 Jiang, H., Yang, X., Cui, Z., Liu, Y., Li, H., Hu, W. & Kloc, C. (2014). *CrystEngComm*, **16**, 5968–5983.

- Kaminska, I., Das, M. R., Coffinier, Y., Niedziolka-Jonsson, J., Woisel, P., Opallo, M., Szunerits, S. & Boukherroub, R. (2012). *Chem. Commun.* **48**, 1221–1223.
- Kobayashi, H., Mori, T., Kato, R., Kobayashi, A., Sasaki, Y., Saito, G. & Inokuchi, H. (1983). *Chem. Lett.* **12**, 581–584.
- Krishnan, R., Binkley, J. S., Seeger, R. & Pople, J. A. (1980). *J. Chem. Phys.* **72**, 650–654.
- Lee, E. C., Kim, D., Jurečka, P., Tarakeshwar, P., Hobza, P. & Kim, K. S. (2007). *J. Phys. Chem. A*, **111**, 3446–3457.
- Lieffrig, J., Jeannin, O., Vacher, A., Lorcy, D., Auban-Senzier, P. & Fourmigué, M. (2014). *Acta Cryst.* **B70**, 141–148.
- Mackie, I. D. & DiLabio, G. A. (2011). *J. Chem. Phys.* **135**, 134318.
- Malenov, D. P., Janjić, G. V., Medaković, V. B., Hall, M. B. & Zarić, S. D. (2017). *Coord. Chem. Rev.* **345**, 318–341.
- Malenov, D. P. & Zarić, S. D. (2018). *Phys. Chem. Chem. Phys.* **20**, 14053–14060.
- Martín, N. (2013). *Chem. Commun.* **49**, 7025–7027.
- Mora, A. J., Belandria, L. M., Delgado, G. E., Seijas, L. E., Lunar, A. & Almeida, R. (2017). *Acta Cryst.* **B73**, 968–980.
- Nielsen, M. B., Lomholt, C. & Becher, J. (2000). *Chem. Soc. Rev.* **29**, 153–164.
- Ninković, D. B., Janjić, G. V., Veljković, D. Ž., Sredojević, D. N. & Zarić, S. D. (2011). *ChemPhysChem*, **12**, 3511–3514.
- Ninković, D. B., Malenov, D. P., Petrović, P. V., Brothers, E. N., Niu, S., Hall, M. B., Belić, M. R. & Zarić, S. D. (2017). *Chem. Eur. J.* **23**, 11046–11053.
- Ninković, D. B., Vojislavljević-Vasilev, D. Z., Medaković, V. B., Hall, M. B., Brothers, E. N. & Zarić, S. D. (2016). *Phys. Chem. Chem. Phys.* **18**, 25791–25795.
- Otsubo, T. & Takimiya, K. (2004). *Bull. Chem. Soc. Jpn.* **77**, 43–58.
- Parrish, R. M., Burns, L. A., Smith, D. G. A., Simmonett, A. S., DePrince, A. E., Hohenstein, E. G., Bozkaya, U., Sokolov, A. Y., Di Remigio, R., Richard, R. M., Gonthier, J. F., James, A. M., McAlexander, H. R., Kumar, A., Saitow, M., Wang, X., Pritchard, B. P., Verma, P., Schaefer, H. F., Patkowski, K., King, R. A., Valeev, E. F., Evangelista, F. A., Turney, J. M., Crawford, T. D. & Sherrill, C. D. (2017). *J. Chem. Theory Comput.* **13**, 3185–3197.
- Raghavachari, K., Trucks, G. W., Pople, J. A. & Head-Gordon, M. A. (1989). *Chem. Phys. Lett.* **157**, 479–483.
- Raju, R. K., Bloom, J. W. G., An, Y. & Wheeler, S. E. (2011). *ChemPhysChem*, **12**, 3116–3130.
- Rosokha, S. V. & Kochi, J. K. (2007). *J. Am. Chem. Soc.* **129**, 828–838.
- Rovira, C. & Novoa, J. J. (1999). *Chem. Eur. J.* **5**, 3689–3697.
- Rubeš, M., Bludský, O. & Nachtigall, P. (2008). *ChemPhysChem*, **9**, 1702–1708.
- Salonen, L. M., Ellermann, M. & Diederich, F. (2011). *Angew. Chem. Int. Ed.* **50**, 4808–4842.
- Segura, J. L. & Martín, N. (2001). *Angew. Chem. Int. Ed.* **40**, 1372–1409.
- Sherrill, C. D. (2013). *Acc. Chem. Res.* **46**, 1020–1028.
- Sinnokrot, M. O. & Sherrill, C. D. (2004). *J. Phys. Chem. A*, **108**, 10200–10207.
- Sinnokrot, M. O., Valeev, E. F. & Sherrill, C. D. (2002). *J. Am. Chem. Soc.* **124**, 10887–10893.
- Varghese, N., Ghosh, A., Voggu, R., Ghosh, S. & Rao, C. N. R. (2009). *J. Phys. Chem. C*, **113**, 16855–16859.
- Wang, F.-F., Wang, Y., Wang, B.-Q., Wang, Y.-F., Ma, F. & Li, Z.-R. (2009). *Sci. China Ser. B Chem.* **52**, 1980–1986.
- Wang, B., Wang, F., Ma, F., Li, Z., Xu, H. & Gu, F. (2011). *Atomic and Molecular Nonlinear Optics: Theory, Experiment and Computation*, edited by G. Maroulis, T. Bancewicz, B. Champagne & A. D. Buckingham, pp. 244–253. IOS Press.
- Weigend, F. & Ahlrichs, R. (2005). *Phys. Chem. Chem. Phys.* **7**, 3297–3305.
- Wudl, F., Wobschall, D. & Hufnagel, E. (1972). *J. Am. Chem. Soc.* **94**, 670–672.
- Yamada, J. & T. Sugimoto, T. (2004). Editors. *TTF Chemistry. Fundamentals and Applications of Tetrathiafulvalene*. Springer Verlag.
- Ziganshina, A. Y., Ko, Y. H., Jeon, W. S. & Kim, K. (2004). *Chem. Commun.* **40**, 806–807.